Impacts of frailty on heart rate variability in aging mice: Roles of the autonomic nervous system and sinoatrial node

Tristan W. Dorey, BSc, Hailey J. Jansen, PhD, Motahareh Moghtadaei, PhD, K. Lockhart Jamieson, PhD, Robert A. Rose, PhD, FHRS

From the Libin Cardiovascular Institute, Department of Cardiac Sciences, Department of Physiology and Pharmacology, Cumming School of Medicine, University of Calgary, Calgary, Alberta, Canada.

BACKGROUND Heart rate variability (HRV) is determined by intrinsic sinoatrial node (SAN) activity and the autonomic nervous system (ANS). HRV is reduced in aging; however, aging is heterogeneous. Frailty, which can be measured using a frailty index (FI), can quantify health status in aging separately from chronological age.

OBJECTIVE The purpose of this study was to investigate the impacts of age and frailty on HRV in mice.

METHODS Frailty was measured in aging mice between 10 and 130 weeks of age. HRV was assessed using time domain, frequency domain, and Poincaré plot analyses in anesthetized mice at baseline and after ANS blockade, as well as in isolated atrial preparations.

RESULTS HRV was reduced in aged mice (90–130 weeks and 50–80 weeks old) compared to younger mice (10–30 weeks old); however, there was substantial variability within age groups. In contrast, HRV was strongly correlated with FI score regardless of chronological age. ANS blockade resulted in reductions in heart rate that were largest in 90- to 130-week-old mice and were correlated with FI score. HRV after ANS blockade or in isolated atrial preparations was increased in aged mice but again showed high variability among age groups. HRV was correlated with FI score after ANS blockade and in isolated atrial preparations.

CONCLUSION HRV is reduced in aging mice in association with a shift in sympathovagal balance and increased intrinsic SAN beating variability; however, HRV is highly variable within age groups. HRV was strongly correlated with frailty, which was able to detect differences in HRV separately from chronological age.

KEYWORDS Aging; Autonomic nervous system; Frailty heart rate; Heart rate variability; Sinoatrial node

(Heart Rhythm 2021;18:1999–2008)

Introduction

Heart rate (HR) is a critical indicator of cardiac performance that is determined by the intrinsic properties of the sinoatrial node (SAN) and modulated by the sympathetic and parasympathetic divisions of the autonomic nervous system (ANS).[1] The sympathetic nervous system (SNS) increases HR by enhancing intrinsic SAN function (via β-adrenergic receptors), whereas the parasympathetic nervous system (PNS) reduces HR by inhibiting the SAN (via muscarinic receptors).[1] It is well recognized that HR exhibits a beat-to-beat variation denoted as heart rate variability (HRV).[2,3] Reduced HRV is associated with increased risk for cardiovascular diseases and mortality, whereas a robust level of HRV is an indicator of a healthy cardiovascular system.[2,4] HRV arises from changes in the activity of the ANS (ie, changes in sympathovagal balance), its effects on SAN activity, and alterations in the intrinsic properties of the SAN.[2,5,6]

The global population continues to experience increased longevity and longer lifespan. With this comes an increasing incidence of cardiac disease due to age-dependent changes in cardiac function.[7,8] SAN dysfunction and impairments in HR regulation are highly prevalent in aging and can occur due to alterations in intrinsic SAN function as well as changes in the ANS and its regulation of the SAN.[9–13] Although aging is a major risk factor for cardiac disease, including SAN dysfunction, it is essential to recognize that not all individuals age at the same rate. This has led to the concept of frailty, which describes an increased susceptibility to adverse health outcomes, including in individuals of similar chronological age.[14] As the global population ages, there is an increasing need to accurately identify individuals who are frail and to distinguish them from those who exhibit

Funding sources: This work was supported by the Heart and Stroke Foundation (G-18-0022148) and the Canadian Institutes of Health Research (MOP 142486 and PJT 166105) to Dr Rose. Tristan W. Dorey holds a Canadian Institutes of Health Research Doctoral Research Award. Dr Jansen holds a Libin Cardiovascular Institute Postdoctoral Fellowship. Dr Jamieson is supported by a Cumming School of Medicine/Libin Cardiovascular Institute Postdoctoral Fellowship. Disclosures: The authors have no conflicts of interest to disclose. **Address reprint requests and correspondence:** Dr Robert A. Rose, Libin Cardiovascular Institute, Cumming School of Medicine, University of Calgary, GAC66, Health Research Innovation Centre, 3280 Hospital Drive NW, Calgary, Alberta, Canada T2N 4Z6. E-mail address: robert.rose@ucalgary.ca.

  https://doi.org/10.1016/j.hrthm.2021.07.069

healthy aging in order to ensure proper care based on the accurate assessment of health status.

Frailty can be quantified using a frailty index (FI), which measures health deficit accumulation over time in aging individuals.[14,15] We developed the mouse clinical FI, which noninvasively quantifies frailty based on 31 established indicators of overall health status.[16] With this approach, the FI score for an individual is measured by determining the ratio between the number of health deficits present and the total number of items assessed. This mouse clinical FI was developed based on similar approaches used in human patients, and it reliably reproduces the major features of deficit accumulation and frailty in aging humans.[14,16] Previous studies demonstrated the ability of the mouse clinical FI to assess health status and heterogeneity in cardiac function in aging mice.[10,17,18]

Although frailty is a powerful approach for assessing overall health status independently of chronological age and HRV is a recognized indicator of cardiovascular health, few studies have investigated the links between frailty and HRV, and none have been conducted using the FI approach. Similarly, the links between intrinsic SAN function, sympathovagal balance, and HRV in aging are incompletely understood. Accordingly, the purpose of this study was to investigate HRV in aging and frail mice, using the mouse clinical FI, *in vivo* and in isolated atrial preparations lacking neural inputs.

Methods

An expanded methods section is available in the Supplemental Methods.

Mice

This study was conducted using male and female wild-type C57Bl/6 mice between the ages of 10 and 130 weeks. All experimental procedures were approved by the University of Calgary Animal Care and Use Committee (protocol AC21-0019) and were in accordance with the guidelines of the Canadian Council on Animal Care as well as the ARRIVE guidelines. As HRV can be affected by environmental conditions,[19] housing conditions for mice were monitored and controlled as explained in the Supplemental Methods.

Frailty assessment

Frailty was assessed using the mouse clinical FI as previously described.[10,16] In brief, specific assessments of the integument, musculoskeletal, vestibulocochlear/auditory, ocular, nasal, digestive, urogenital, and respiratory systems were performed. Signs of discomfort, body temperature, and body mass were assessed. Each item was given a score of 0 (no sign of deficit), 0.5 (mild deficit), or 1 (severe deficit). Deficits in body temperature and body mass were scored based on deviation from the mean in all mice. The scores for each item were added together, and the sum was divided by the number of items measured (ie, 31 items) to yield an FI score between 0 and 1.

In vivo HR monitoring

HR was measured in anesthetized mice as described previously [10,20,21] and in the Supplemental Methods.

Electrogram recordings in isolated atrial preparations

Electrograms were recorded in spontaneously beating, intact, denervated atrial preparations containing the SAN as described previously [6,20] and in the Supplemental Methods.

HRV analysis

HRV was assessed *in vivo* and in isolated atrial preparations using time-domain and frequency-domain analysis, as well as nonlinear metrics from Poincaré plots as described previously [6,22,23] and in the Supplemental Methods.

Statistical analysis

Summary data comparing distinct age groups are given as mean ± SEM. Sample sizes for all experimental groups were selected in accordance with previous studies demonstrating groups sizes used for frailty studies.[10,17] Normality was tested using a Shapiro-Wilk test. Normally distributed data were analyzed using 1-way analysis of variance with a Holm-Sidak *post hoc* test. Nonparametric data were analyzed using a Kruskal-Wallis test with Dunn *post hoc* test. Specific statistical tests and n values are reported in each figure legend. Frailty analyses were performed using linear regressions (shown with 95% confidence intervals) and Pearson correlation to obtain correlation coefficients. $P < .05$ was considered significant.

Results

Frailty in aging mice

FI scores were measured in wild-type mice divided into 3 age groups: 10–30 weeks (10–30wk), 50–80 weeks (50–80wk), and 90–130 weeks (90–130wk). On average, FI scores increased progressively across these age groups (Figure 1A). There was also substantial variability within each age group (Figure 1A). As a result, FI scores exhibit overlap, indicating that mice in the different age groups can have similar "health status" regardless of chronological age differences. Thus, health status can be distinguished by frailty assessment separately from chronological age.

Effects of age and frailty on HRV *in vivo*

Representative RR-interval tachograms (Figure 1B) and RR-interval histograms (Figure 1C) demonstrate that RR interval was longer in 90–130wk mice compared to 10–30wk mice, indicating lower HR in aged mice. When comparing distinct age cohorts, RR interval was longer in 50–80wk and 90–130wk mice compared to 10–30wk mice; however, no differences were detected between 50–80wk and 90–130wk mice

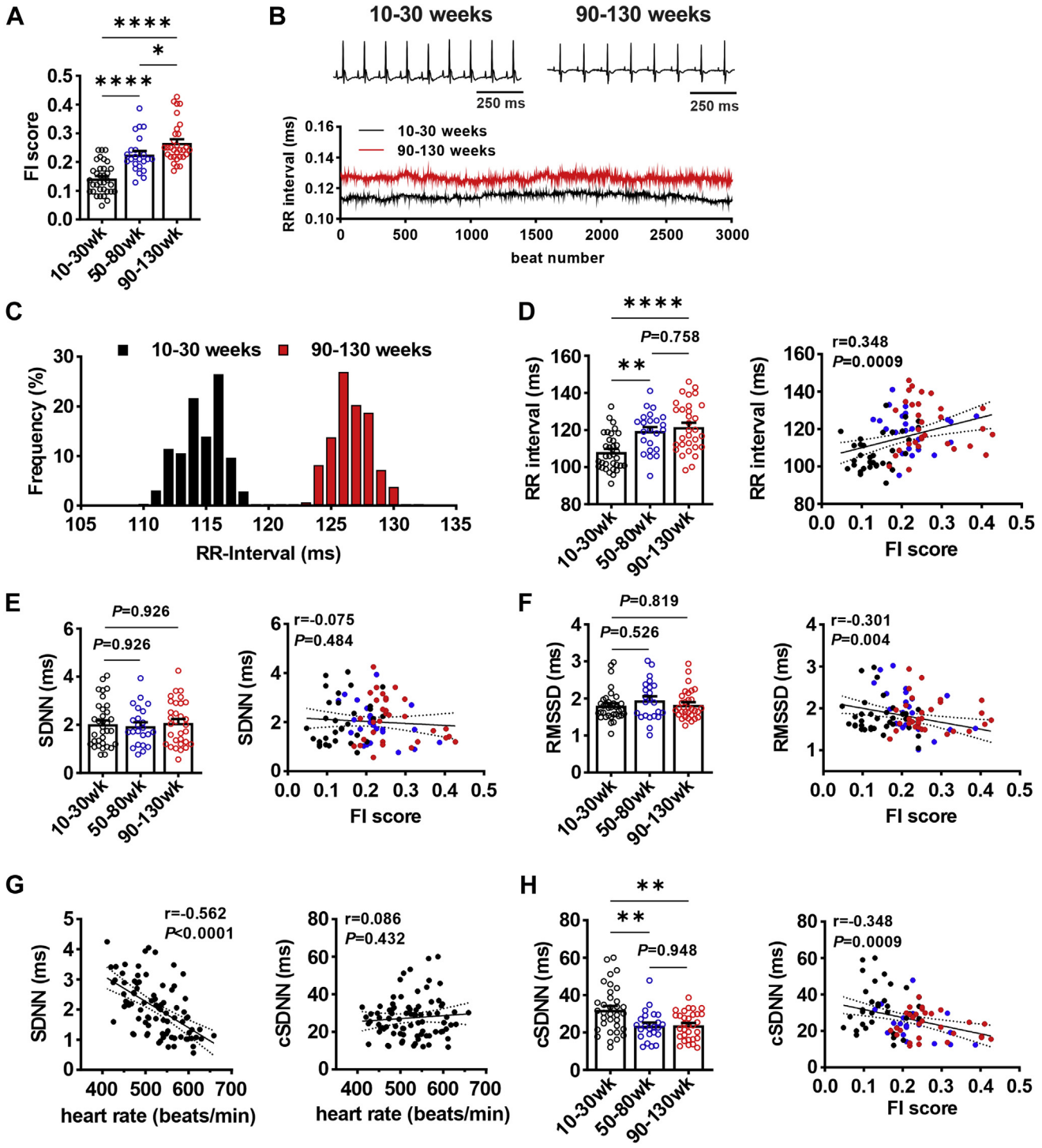

Figure 1 Time-domain analysis of heart rate variability in aging and frail mice *in vivo*. **A:** Summary of frailty index (FI) scores based on chronological age groups. **B:** Representative electrocardiographic recordings and tachograms for 10- to 30-week-old and 90- to 130-week-old mice. **C:** Representative RR-interval histograms for 10-to 30-week-old and 90- to 130-week-old mice. **D–F:** Summary of differences in RR interval **(D)**, standard deviation of all normal RR intervals (SDNN) **(E)**, and root mean square of successive differences in RR interval (RMSSD) **(F)** as a function of chronological age **(left)** and FI score **(right)**. In each panel, the same mice were analyzed as a function of age group and FI score as indicated by the colors. **G:** Linear regression analysis of SDNN **(left)** and corrected SDNN (cSDNN) **(right)** as a function of heart rate for all animals studied. **H:** Summary of cSDNN as a function of chronological age **(left)** and FI score **(right)**. For bar graphs: $*P < .05$, $**P < .01$, $****P < .0001$ by 1-way analysis of variance with Holm-Sidak *post hoc* test. Linear regressions analyzed using Pearson correlation. n = 34 for 10- to 30-week-old mice; n = 23 for 50- to 80-week-old mice; and n = 31 for 90- to 130-week-old mice.

(Figure 1D). When RR interval was measured as a function of FI score in the same mice, RR interval fell along a continuum and was correlated with FI score (Figure 1D). From this analysis, it is evident that mice that had similar FI scores also had similar RR intervals regardless of chronological age. Thus, RR interval was graded by FI score in aging mice.

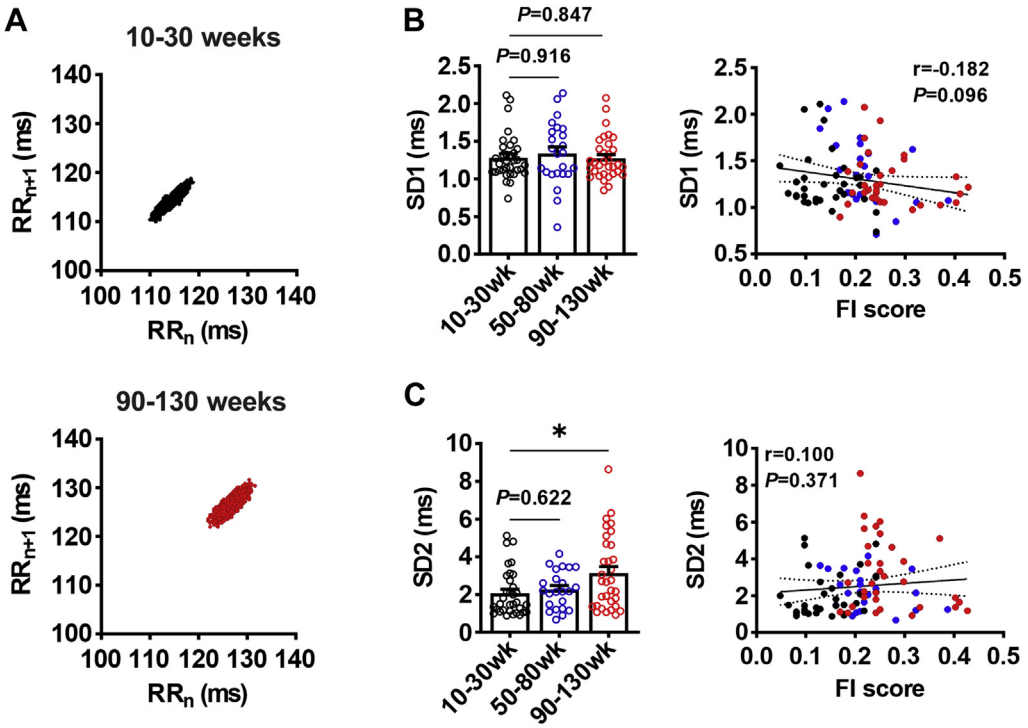

Figure 2 Nonlinear metrics of heart rate variability in aging and frail mice *in vivo*. **A:** Representative Poincaré plots from 10- to 30-week-old and 90- to 130-week-old mice. **B, C:** Summary of standard deviations including SD1 **(B)** and SD2 **(C)**, as a function of chronological age **(left)** and FI score **(right)**. For bar graphs: **P* <.05 by 1-way analysis of variance with Holm-Sidak *post hoc* test. Linear regressions analyzed using Pearson correlation. n = 34 for 10- to 30-week-old mice; n = 23 for 50- to 80-week-old mice; and n = 31 for 90- to 130-week-old mice.

No differences were seen in the standard deviation of RR intervals (SDNN) in anesthetized mice as a function of age or FI score (Figure 1E). There also were no differences in the root mean square of successive differences (RMSSD) when comparing discrete age groups (Figure 1F). When analyzed as a function of frailty, RMSSD was negatively correlated with FI score (Figure 1F). HR itself, which is reduced in aged mice, has an important effect on overall HRV[22]; therefore, SDNN was corrected for HR (see Methods). Linear regression analysis of the relationship between HR and SDNN yields an r^2 value of 0.317, indicating that HR accounts for ~32% of the variation in SDNN in these mice (Figure 1G). Corrected SDNN (cSDNN) showed no correlation with HR (Figure 1G). cSDNN was reduced in 50–80wk and 90–130wk mice compared to 10–30wk mice; however, no differences were detected between 50–80wk and 90–130wk mice (Figure 1H). cSDNN showed a negative correlation with FI score (Figure 1H).

HRV was also assessed from standard deviations (ie, SD1 and SD2) from Poincaré plots for RR intervals (Figure 2A). No differences in SD1 were observed when comparing discrete age groups, whereas there was a trend (P = .096) toward reduced SD1 when measured as a function of FI score (Figure 2B). SD2 was increased in 80–130wk mice compared to 10–30wk mice, but other differences were not detected between discrete age groups (Figure 2C), and SD2 was not correlated with FI score (Figure 2C).

Frequency-domain measures of HRV were assessed from power spectral density plots (Figure 3A). No differences in total power were observed when comparing age groups (Figure 3B). When analyzed as a function of frailty, total power was negatively correlated with FI score (Figure 3B). Very-low-frequency (VLF) power was reduced in 90–130wk vs 10–30wk mice, but other differences among discrete groups were not observed (Figure 3C). VLF was also negatively correlated with FI score (Figure 3C). Low-frequency (LF) power tended to be lower (P = .087) in 90–130wk mice compared to 10–30wk mice, but no other differences were detected between age groups (Figure 3D). LF power was reduced and graded by FI score (Figure 3D). No differences in high-frequency (HF) power were observed when comparing discrete age groups, but HF power was negatively correlated with FI score (Figure 3E).

HR and HRV during ANS blockade *in vivo*

To assess intrinsic SAN function and its impacts on HR and HRV *in vivo*, anesthetized mice were injected with atropine and propranolol to block the ANS. ANS blockade resulted in an increase in RR interval (Figure 4A). This increase in RR interval was larger in 90–130wk mice compared to both 10–30wk and 50–80wk and was not different between 50–80wk mice and 10–30wk mice (Figure 4B). The change in RR interval produced by ANS blockade was positively correlated with FI score (Figure 4B).

Representative RR-interval histograms after ANS blockade demonstrate that RR interval was longer and

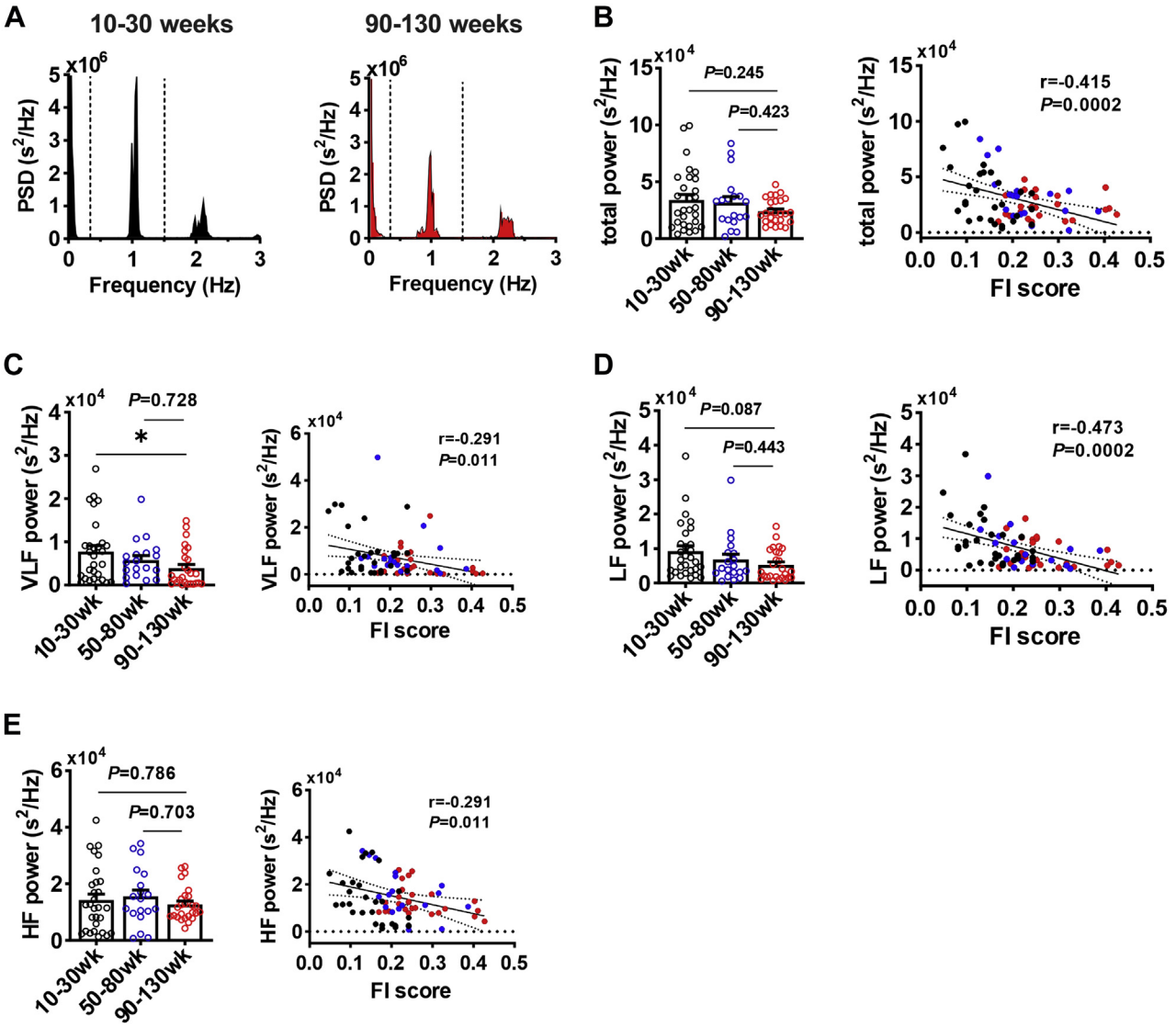

Figure 3 Frequency domain analysis of heart rate variability in aging and frail mice *in vivo*. **A:** Representative power spectral density curves from 10- to 30-week-old and 90- to 130-week-old mice. **B–E:** Summary of total power **(B)**, very-low-frequency (VLF) power **(C)**, low-frequency (LF) power **(D)**, and high-frequency (HF) power **(E)** as a function of chronological age **(left)** and frailty index (FI) score **(right)**. For bar graphs: **P* <.05 by Kruskal-Wallis test with Dunn *post hoc* test. Linear regressions analyzed using Pearson correlation. n = 34 for 10-to 30-week-old mice; n = 23 for 50- to 80-week-old mice; and n = 31 for 90- to 130-week-old mice.

more variable in 90–130wk mice compared to 10–30wk mice (Figure 5A). Summary data confirm that RR interval was longer in 90–130wk vs 10–30wk mice following ANS blockade; however, differences among other age groups were not observed (Figure 5B). In addition, RR interval after ANS blockade was positively correlated with, and graded by, FI score.

SDNN and RMSSD were each increased in 90–130wk mice compared to both 10–30wk and 50–80wk mice after ANS blockade, whereas no differences were observed between 50–80wk mice and 10–30wk mice (Figures 5C and 5D). When quantified as a function of health status, SDNN and RMSSD were each positively correlated with FI score (Figures 5C and 5D).

HRV following ANS blockade was also measured using Poincaré plots (Figure 6A). SD1 after ANS blockade was increased in 90–130wk mice compared to 10–30wk mice, but other differences were not observed when comparing distinct age groups (Figure 6B). In addition, SD1 was increased as a function of FI score after ANS blockade (Figure 6B). SD2 was increased in 90–130wk mice compared to younger age groups following ANS blockade; however, differences were not observed between 50–80wk and 10–30wk mice (Figure 6C). Frailty analysis shows that SD2 was positively correlated with FI score following ANS blockade (Figure 6C).

Beating rate variability in isolated atrial preparations

Isolated atrial preparations lacking neural input were used to further investigate the role of intrinsic SAN function in

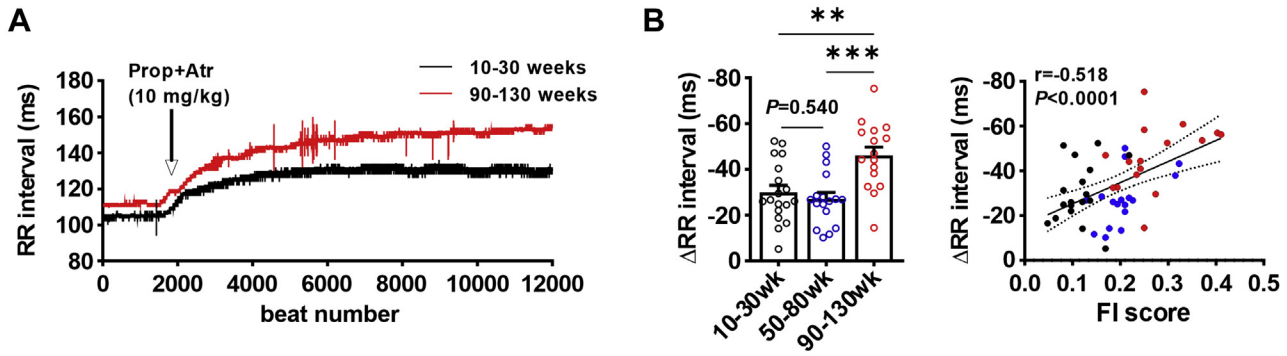

Figure 4 Effects of autonomic nervous system (ANS) blockade on RR interval in aging and frail mice *in vivo*. **A:** Representative data illustrating the effects of ANS blockade on RR interval in 10- to 30-week-old and 90- to 130-week-old mice. ANS blockade was elicited using a combined injection of propranolol (Prop; 10 mg/kg) and atropine (Atr; 10 mg/kg). **B:** Summary of the change (Δ) in RR interval following ANS blockade as a function of chronological age **(left)** and frailty index (FI) score **(right)**. For bar graph: $^{**}P < .01$, $^{***}P < .001$ by 1-way analysis of variance with Holm-Sidak *post hoc* test. Linear regressions analyzed using Pearson correlation. n = 18 for 10- to 30-week-old mice; n = 17 for 50- to 80-week-old mice; and n = 16 for 90-to 130-week-old mice.

beating rate and beating rate variability in aging and frail mice. Representative electrograms and tachograms demonstrate that NN interval was longer (ie, beating rate was slower) and more variable in atrial preparations from 90–130wk mice compared to 10–30wk mice (Figure 7A). On average, NN interval was increased in 90–130wk atrial preparations compared to both younger age groups; however, no differences were detected between 50–90wk and 10–30wk atrial preparations (Figure 7B). NN interval in isolated atrial preparations was positively correlated with FI score (Figure 7B).

SDNN and RMSSD were each increased between 50–80wk and 10–30wk as well as between 90–130wk and 10–30wk atrial preparations; however, differences were not detected between 90–130wk and 50–90wk atrial preparations (Figures 7C and 7D). SDNN and RMSSD were each graded along a continuum when measured as a function of FI score (Figures 7C and 7D).

Poincaré plot analysis of NN intervals in isolated atrial preparations (Figure 8A) demonstrates that SD1 was increased in 90–130wk and 50–80wk atrial preparations compared to 10–30wk atrial preparations (Figure 8B). Conversely, no differences were detected between 90–130wk and 50–80wk atrial preparations (Figure 8B). Frailty analysis revealed that SD1 was correlated with, and graded by, FI score across all age groups (Figure 8B). Similar observations were made for SD2 when analyzed as a function of age group as well as FI score (Figure 8C).

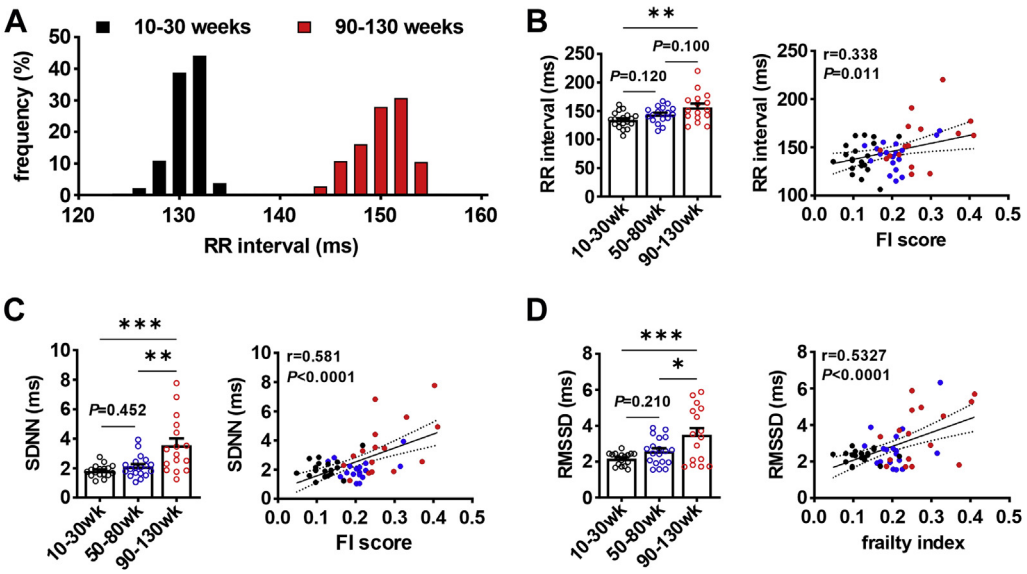

Figure 5 Time-domain analysis of heart rate variability in aging and frail mice *in vivo* following autonomic nervous system (ANS) blockade. **A:** Representative RR interval histogram for 10-to 30-week-old and 90- to 130-week-old mice following ANS blockade. **B–D:** Summary of RR interval **(B)**, standard deviation of RR intervals (SDNN) **(C)**, and root mean square of successive differences in RR interval (RMSSD) **(D)** as a function of chronological age **(left)** and frailty index (FI) score **(right)**. For bar graphs: $^{*}P < .05$, $^{**}P < .01$, $^{***}P < .001$ by 1-way analysis of variance with Holm-Sidak *post hoc* test **(B, D)** or Kruskal-Wallis test with Dunn *post hoc* test **(C).** Linear regressions analyzed using Pearson correlation. n = 18 for 10- to 30-week-old mice; n = 17 for 50- to 80-week-old mice; and n = 16 for 90- to 130-week-old mice.

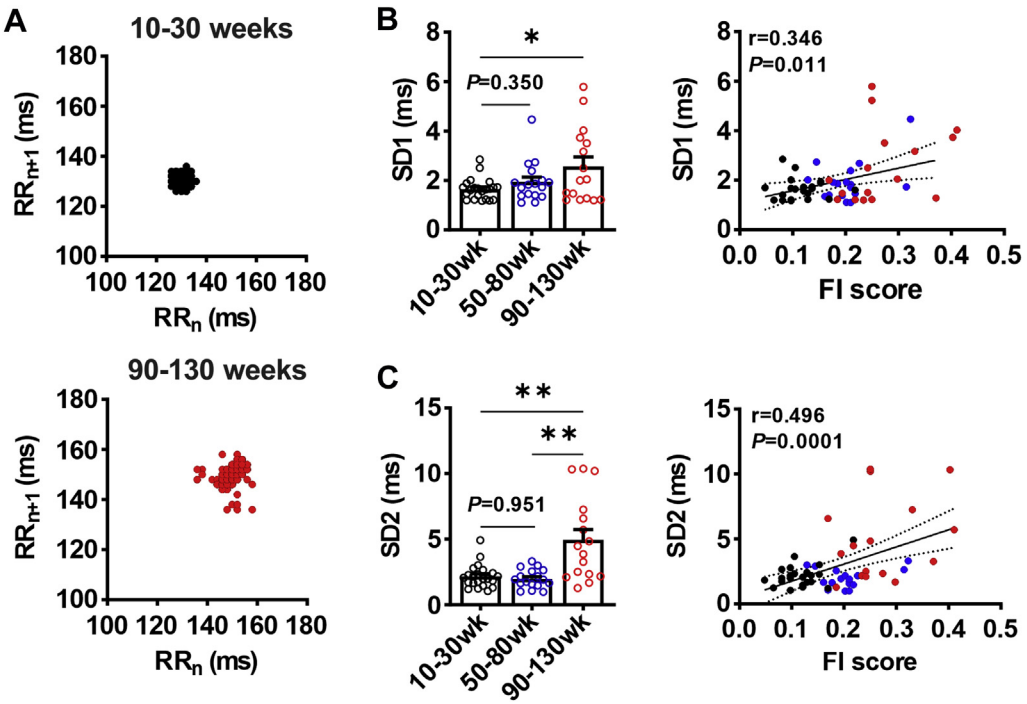

Figure 6 Nonlinear metrics of heart rate variability in aging and frail mice following autonomic nervous system (ANS) blockade. **A:** Representative Poincaré plots from 10- to 30-week-old and 90- to 130-week-old mice after ANS blockade. **B, C:** Summary of SD1 **(B)** and SD2 **(C)** as a function of chronological age **(left)** and frailty index (FI) score **(right)**. For bar graphs: $*P < .05$, $**P < .01$ by Kruskal-Wallis test with Dunn *post hoc* test. Linear regressions analyzed using Pearson correlation. n = 18 for 10- to 30-week-old mice; n = 17 for 50- to 80-week-old mice; and n = 16 for 90- to 130-week-old mice.

Discussion

This study demonstrates that aging results in reduced HRV *in vivo*, as well as increased intrinsic SAN beating interval variability, and that each of these is strongly associated with frailty (ie, health status). Three distinct age groups were used in the present study and, although aging clearly led to reduced HRV, differences among all 3 discrete age groups were not always detected. This is likely related to the variability in frailty (ie, health status), as well as measures of HRV, within each age group. Specifically, FI score increased progressively with age; however, there was also substantial variability in FI score within age groups, indicating that mice of different chronological ages could have similar health statuses. Importantly, most measures of HRV were graded on a continuum as a function of FI score. Thus, the data in this study consistently show that mice that have similar FI scores also have similar measures of HRV, regardless of chronological age. This demonstrates the ability of the mouse clinical FI to accurately quantify health status and the associations between measures of HRV and frailty in aging mice. Thus, frailty assessment can importantly supplement studies of the effects of aging on HRV by accounting for variability within mice of similar chronological age.

The mouse clinical FI quantifies overall health status by assessing general indicators of health across several organ systems.[10,16,17] Importantly, the specific items measured are not critical. Rather, the FI approach depends on having a minimum number of items in the index (~30 items). These items need to be associated with health status, increase in prevalence with aging, and cover a range of organ systems, which ensures that the FI very accurately determines overall health status.[14–16] The items in the mouse clinical FI meet all of these criteria.[16]

Changes in resting HR and HRV are commonly used indices of cardiac control by the ANS.[2] Age-dependent reductions in HR and HRV occur due to a combination of impaired ANS function as well as intrinsic SAN dysfunction.[12] This leads to declines in overall cardiac performance as well as an increased risk of critical illness.[24] Consistent with other human and animal studies,[11,25,26] we found that aging results in impaired HR regulation, evident by prolonged RR intervals *in vivo* as well as a slowing of intrinsic SAN beating rate.

Although previous studies reported reductions in HRV with age,[27,28] large datasets often are required to identify significant differences between age groups due to the substantial heterogeneity in aged populations. This can limit the prognostic value of HRV. Consistent with this, differences between distinct age groups for many measures of HRV often were not observed in our study, which could be due to the heterogeneity observed within each group. Specifically, differences between distinct age groups for time-domain metrics such as SDNN and RMSSD, which provide information on general variability and PNS-driven variability,[3] respectively, were not observed. Nevertheless, a significant negative correlation was present when RMSSD was assessed as a function of FI score in the same mice, suggesting reductions in PNS regulation of the SAN as frailty increases and health status declines. Furthermore,

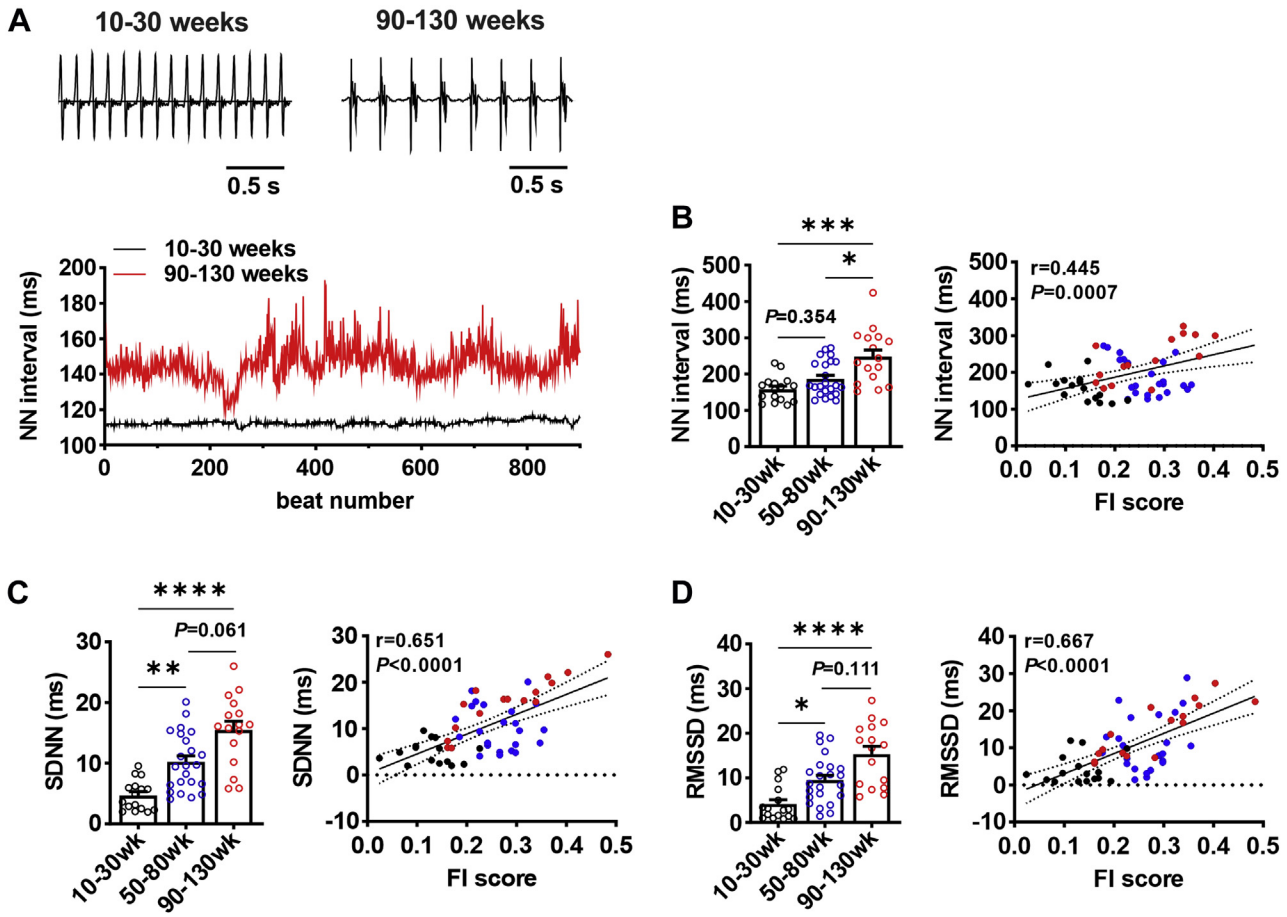

Figure 7 Time-domain analysis of beating rate variability in isolated atrial preparations from aging and frail mice. **A:** Representative electrograms and RR-interval tachogram for isolated atrial preparations from 10- to 30-week-old and 90- to 130-week-old mice. **B–D:** Summary of NN interval **(B)**, standard deviation of RR intervals (SDNN) **(C)**, and root mean square of successive differences in RR interval (RMSSD) **(D)** as a function of chronological age **(left)** and frailty index (FI) score **(right)**. For bar graphs: *P <.05, **P <.01, ***P <.001, ****P <.0001 by Kruskal-Wallis test with Dunn *post hoc* test. Linear regressions analyzed using Pearson correlation. n = 16 for 10- to 30-week-old mice; n = 23 for 50- to 80-week-old mice; and n = 16 for 90- to 130-week-old mice.

when corrected for HR, significant reductions in SDNN that were graded by FI score also became apparent, confirming that HR must be accounted for in time-domain analysis of HRV.[29] *In vivo* SD1 measurements from Poincaré plots provide an assessment of short-term HRV that often correlates with RMSSD.[3] Similar to RMSSD, differences in SD1 were not observed when comparing distinct age groups, but SD1 did show a clear trend toward a reduction as a function of FI score.

In the elderly, altered ANS function may contribute to the progression of frailty and impaired ability to adapt to environmental stimuli.[13] Spectral frequency-domain analysis of the RR-interval time series is commonly used to assess cardiovascular regulation by the ANS. HF power largely represents phasic PNS control of HR, whereas LF power represents a combination of SNS and PNS influences.[3] VLF power is thought to represent reflex changes in HR due to long-term blood pressure regulatory mechanisms.[3] Similar to time-domain analysis, few differences were observed in spectral HRV metrics when comparing distinct age groups. However, all frequency-domain analyses demonstrated strong negative correlations with FI score, which is consistent with the findings from time-domain analyses. Collectively, this suggests an overall shift in ANS activity toward enhanced SNS signaling with increasing frailty.

The intrinsic properties of the SAN can also alter HRV *in vivo*.[5,6,12] SAN disease is highly prevalent in aging populations,[9,10] which needs to be considered when interpreting HRV as a measure of ANS function. This study is consistent with other studies, which demonstrate that changes in intrinsic SAN beating interval variability in aging contribute to overall HRV.[12,30] Specifically, we found that beating interval variability under ANS blockade and in isolated atrial preparations was significantly increased in aged mice when assessed using time-domain analyses and Poincaré plots. Moreover, beating rate variability was highly associated with FI score, consistent with our previous study showing that SAN function is affected by frailty in aging mice.[10] This, in conjunction with the reduced HRV observed in frail anesthetized mice, supports the idea that sympathovagal balance must shift toward increased sympathetic activity to compensate for impaired SAN function in aging. Consistent with this, the change in RR interval following ANS blockade was also graded as a function of frailty. More frail animals

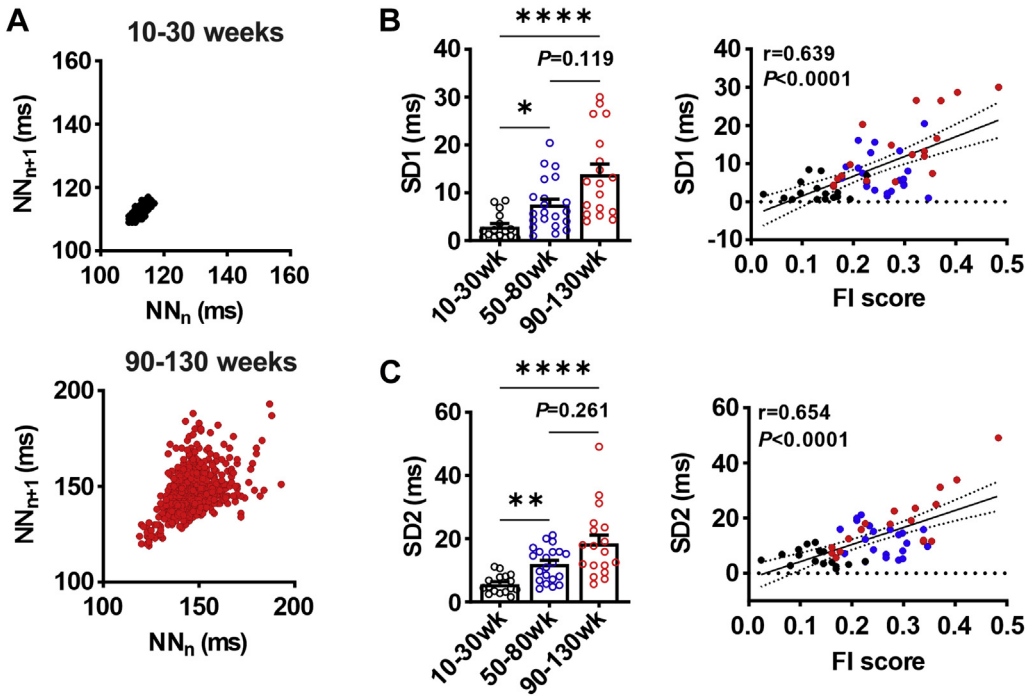

Figure 8 Nonlinear metrics of beating rate variability in isolated atrial preparations from aging and frail mice. **A:** Representative Poincaré plots from isolated atrial preparations from 10- to 30-week-old and 90- to 130-week-old mice. **B, C:** Summary of SD1 **(B)** and SD2 **(C)** as a function of chronological age **(left)** and frailty index (FI) score **(right)**. For bar graphs: *$P < .05$, **$P < .01$, ****$P < .0001$ by Kruskal-Wallis test with Dunn *post hoc* test. Linear regressions analyzed using Pearson correlation. n = 16 for 10- to 30-week-old mice; n = 21 for 50- to 80-week-old mice; and n = 18 for 90- to 130-week-old mice.

had larger changes in RR interval, indicating increased sympathetic regulation of HR.

Some previous studies have assessed the relationship between frailty and HRV but have used different approaches that define frailty as a phenotype that is either present or absent.[31] Although still informative, these studies do not enable the quantitative analysis that can be obtained using a FI, which more effectively facilitates the differentiation of health status among individuals and how it relates to HRV. Collectively, these data demonstrate that frailty (ie, health status) accurately predicts an individual's HRV as a function of health status separately from chronological age.

Study limitations

Although our study provides insight into the relationships between age, frailty, and autonomic cardiovascular control, some limitations should be noted. Mice exhibit differences in resting ANS activity compared to humans.[32] As such, future studies will be required to determine the links between age, frailty, and HRV (including the role of intrinsic SAN function) in humans. In addition, in our study, the impacts of age on HRV were assessed by comparing discrete age groups, whereas frailty, which fell along a continuum, was analyzed by linear regression. In future studies, the impacts of age could also be investigated using ages along a full continuum from youngest to oldest. Combining this with frailty assessment would facilitate the ability to use multiple regression analyses, which would enable the assessment of the relative contributions of chronological age and frailty to changes in HRV in aging mice.

Conclusion

This study provides a comprehensive assessment of the relationships between age, frailty, and multilevel HRV. The data presented highlight that age-dependent changes in HRV can exhibit substantial variability and that changes in HRV can be accurately discriminated based on frailty (ie, overall health status). Furthermore, we show that although HRV is reduced in a frailty-dependent manner during aging, SAN beating rate variability increases with both age and frailty status. Therefore, sympathovagal balance must shift to maintain HR *in vivo*, which contributes to reduced HRV. These findings further our understanding of the relationship between intrinsic SAN function, the ANS, and HRV. Understanding the impacts of age and frailty on HRV is of substantial clinical importance because it can help identify patients who may be more susceptible to adverse outcomes or who are better able to tolerate interventions and procedures. Thus, frailty assessment in combination with HRV measurements may lead to more effective decision-making for aged patients with cardiovascular disease.

Acknowledgment

We thank Sara Rafferty for outstanding technical assistance.

Appendix

Supplementary data

Supplementary data associated with this article can be found in the online version at https://doi.org/10.1016/j.hrthm.2021.07.069.

References

1. MacDonald EA, Rose RA, Quinn TA. Neurohumoral control of sinoatrial node activity and heart rate: insight from experimental models and findings from humans. Front Physiol 2020;11:170.
2. Billman GE. Heart rate variability—a historical perspective. Front Physiol 2011; 2:86.
3. Shaffer F, Ginsberg JP. An overview of heart rate variability metrics and norms. Front Publ Health 2017;5:258.
4. Hillebrand S, Gast KB, de Mutsert R, et al. Heart rate variability and first cardiovascular event in populations without known cardiovascular disease: meta-analysis and dose-response meta-regression. Europace 2013;15:742–749.
5. Yaniv Y, Lyashkov AE, Lakatta EG. Impaired signaling intrinsic to sinoatrial node pacemaker cells affects heart rate variability during cardiac disease. J Clin Trials 2014;4.
6. Dorey TW, Moghtadaei M, Rose RA. Altered heart rate variability in angiotensin II-mediated hypertension is associated with impaired autonomic nervous system signaling and intrinsic sinoatrial node dysfunction. Heart Rhythm 2020; 17:1360–1370.
7. Alfaras I, Di Germanio C, Bernier M, et al. Pharmacological strategies to retard cardiovascular aging. Circ Res 2016;118:1626–1642.
8. Lakatta EG, Levy D. Arterial and cardiac aging: major shareholders in cardiovascular disease enterprises: part II: the aging heart in health: links to heart disease. Circulation 2003;107:346–354.
9. Dobrzynski H, Boyett MR, Anderson RH. New insights into pacemaker activity: promoting understanding of sick sinus syndrome. Circulation 2007; 115:1921–1932.
10. Moghtadaei M, Jansen HJ, Mackasey M, et al. The impacts of age and frailty on heart rate and sinoatrial node function. J Physiol 2016;594:7105–7126.
11. Larson ED, St Clair JR, Sumner WA, Bannister RA, Proenza C. Depressed pacemaker activity of sinoatrial node myocytes contributes to the age-dependent decline in maximum heart rate. Proc Natl Acad Sci U S A 2013; 110:18011–18016.
12. Yaniv Y, Ahmet I, Tsutsui K, et al. Deterioration of autonomic neuronal receptor signaling and mechanisms intrinsic to heart pacemaker cells contribute to age-associated alterations in heart rate variability in vivo. Aging Cell 2016; 15:716–724.
13. Parashar R, Amir M, Pakhare A, Rathi P, Chaudhary L. Age related changes in autonomic functions. J Clin Diagn Res 2016;10:CC11–CC15.
14. Rockwood K, Blodgett JM, Theou O, et al. A frailty index based on deficit accumulation quantifies mortality risk in humans and in mice. Sci Rep 2017;7:43068.
15. Searle SD, Mitnitski A, Gahbauer EA, Gill TM, Rockwood K. A standard procedure for creating a frailty index. BMC Geriatr 2008;8:24.
16. Whitehead JC, Hildebrand BA, Sun M, et al. A clinical frailty index in aging mice: comparisons with frailty index data in humans. J Gerontol A Biol Sci Med Sci 2014;69:621–632.
17. Jansen HJ, Moghtadaei M, Mackasey M, et al. Atrial structure, function and arrhythmogenesis in aged and frail mice. Sci Rep 2017;7:44336.
18. Feridooni HA, Kane AE, Ayaz O, et al. The impact of age and frailty on ventricular structure and function in C57BL/6J mice. J Physiol 2017; 595:3721–3742.
19. Axsom JE, Nanavati AP, Rutishauser CA, et al. Acclimation to a thermoneutral environment abolishes age-associated alterations in heart rate and heart rate variability in conscious, unrestrained mice. Geroscience 2020;42:217–232.
20. Mackasey M, Egom EE, Jansen HJ, et al. Natriuretic peptide receptor-C protects against angiotensin II-mediated sinoatrial node disease in mice. JACC Basic Transl Sci 2018;3:824–843.
21. Bohne LJ, Jansen HJ, Daniel I, et al. Electrical and structural remodeling contribute to atrial fibrillation in type 2 diabetic db/db mice. Heart Rhythm 2021;18:118–129.
22. Moghtadaei M, Langille E, Rafferty SA, Bogachev O, Rose RA. Altered heart rate regulation by the autonomic nervous system in mice lacking natriuretic peptide receptor C (NPR-C). Sci Rep 2017;7:17564.
23. Dorey TW, Mackasey M, Jansen HJ, et al. Natriuretic peptide receptor B maintains heart rate and sinoatrial node function via cyclic GMP-mediated signaling. Cardiovasc Res 2021 Jul 17; https://doi.org/10.1093/cvr/cvab245.
24. Ogliari G, Mahinrad S, Stott DJ, et al. Resting heart rate, heart rate variability and functional decline in old age. CMAJ 2015;187:E442–E449.
25. Jones SA, Lancaster MK, Boyett MR. Ageing-related changes of connexins and conduction within the sinoatrial node. J Physiol 2004;560:429–437.
26. Christou DD, Seals DR. Decreased maximal heart rate with aging is related to reduced {beta}-adrenergic responsiveness but is largely explained by a reduction in intrinsic heart rate. J Appl Physiol (1985) 2008;105:24–29.
27. Jandackova VK, Scholes S, Britton A, Steptoe A. Are changes in heart rate variability in middle-aged and older people normative or caused by pathological conditions? Findings from a large population-based longitudinal cohort study. J Am Heart Assoc 2016;5:e002365.
28. Almeida-Santos MA, Barreto-Filho JA, Oliveira JL, et al. Aging, heart rate variability and patterns of autonomic regulation of the heart. Arch Gerontol Geriatr 2016;63:1–8.
29. Billman GE. The effect of heart rate on the heart rate variability response to autonomic interventions. Front Physiol 2013;4:222.
30. Yaniv Y, Lyashkov AE, Lakatta EG. The fractal-like complexity of heart rate variability beyond neurotransmitters and autonomic receptors: signaling intrinsic to sinoatrial node pacemaker cells. Cardiovasc Pharm Open Access 2013;2:111.
31. Parvaneh S, Howe CL, Toosizadeh N, et al. Regulation of cardiac autonomic nervous system control across frailty statuses: a systematic review. Gerontology 2015;62:3–15.
32. Shusterman V, Usiene I, Harrigal C, et al. Strain-specific patterns of autonomic nervous system activity and heart failure susceptibility in mice. Am J Physiol Heart Circ Physiol 2002;282:H2076–H2083.

The impacts of frailty on heart rate variability in aging mice: roles of the autonomic nervous system and sinoatrial node

Supplemental Material

Supplemental Methods

Mice

This study was conducted using male and female wild-type C57Bl/6 mice between the ages of 10 and 130 weeks of age. Mice were bred locally in our animal facility and then aged up to 130 weeks. Mice were housed in groups of 3-5 per cage using Tecniplast Green Line GM500 cages with 500 cm^2 of floor space and provided with enrichment items (nesting material, houses) in the cages. Mice were provided with standard rodent chow (LabDiet 5062) and water ad libitum. Mice were kept on a 12:12 hour light:dark cycle. Temperature in the room was maintained at 21-21.5°C and humidity was 32-38%. These environmental and housing conditions were monitored daily and maintained throughout the study.

FI scores were measured in wildtype mice divided into three age groups including 10-30 weeks of age (10-30wk), 50-80 weeks of age (50-80wk) and 90-130 weeks of age (90-130wk). All experiments to measure heart rate and heart rate variability *in vivo* and in isolated atrial preparations were performed with the experimenter blinded to the FI score for each mouse. No mice that were used experimentally were excluded from the study. No differences in FI scores or measures of HRV were seen between males and females; therefore, data were combined.

In-vivo heart rate monitoring

HR was measured in anaesthetized mice (2% isoflurane inhalation) using 30-gauge subdermal needle electrodes (Grass Technologies, Quincy, Massachusetts) in a lead II ECG configuration. Data were acquired using a Gould ACQ-7700 amplifier and Ponemah Physiology Platform software (Data Sciences International, St. Paul, Minnesota). Body temperature was

continuously monitored using a rectal probe and maintained at 37°C with a heating pad. Mice were given 20 min to acclimate before data recording began.

Electrogram recordings in isolated atrial preparations

Mice were administered a 0.2 ml intraperitoneal injection of heparin (1000 IU/ml) to prevent blood clotting and were then anesthetized by isoflurane inhalation and cervically dislocated. Hearts were rapidly excised into Krebs solution (37°C) containing (in mM): 118 NaCl, 4.7 KCl, 1.2 KH_2PO_4, 12.2 $MgSO_4$, 1 $CaCl_2$, 25 $NaHCO_3$, 11 glucose. This Krebs solution was bubbled with 95% O2/5% CO2 to maintain a pH of 7.4. The atria were dissected away from the ventricles and pinned in a dish with the endocardial surface facing upwards. The superior and inferior vena cavae were cut open so that the crista terminalis and the right atrial posterior wall, which contains the SAN, could be visualized.

Electrograms (EGMs) were measured in these isolated atrial preparations using needle electrodes (Grass Technologies, Quincy, Massachusetts) placed in each atrial appendage. Atrial preparations were given 15 min to stabilize before data recording began.

HRV analysis

All HRV data were analyzed using customized software written in MATLAB (MathWorks, Natick, Massachusetts). HRV was assessed using time and frequency domain analysis from anesthetized ECG recordings *in vivo*. Stationary NN interval time series of at least 5 min in duration were used for time domain analysis. Each episode was examined to ensure a stationary and stable sinus rhythm with no trend or periodic fluctuations. Next, R wave detection was performed, and RR interval time series were obtained. In isolated atrial preparations, NN intervals were defined as the interval between peaks on the electrogram recordings in atrial preparations. The time domain parameters we are reporting include the standard deviation of all

normal RR intervals (SDNN, in ms) and the root mean square differences between successive RR intervals (RMSSD, in ms).

To correct for the influence of HR on SDNN, we plotted SDNN as a function of HR for all baseline data and fitted these data with an exponential function, which was then used to generate the following equation to correct for HR and produce corrected SDNN (cSDNN).

$$cSDNN = \frac{SDNN}{e^{-0.004 \times HR}}$$

For frequency domain analysis, each of the day/night, low/high-activity phases were divided into 2 min episodes. These time frames were chosen in order to ensure that each episode contained at least 1024 data points (R waves). Similar to the time domain analysis, each episode was manually examined to ensure a stationary and stable sinus rhythm, which is required for performing fast Fourier transforms (see below). Next, R wave detection was performed, and the RR interval time series were generated. Linear trends and drift were removed from the signal to reveal the HRV in the data. In the present study, we have used Welch's method to characterize the frequency content of the signal, i.e., to estimate the power of the signal at different frequencies. In Welch's method, the signal is broken into overlapping segments to reduce noise in the frequency spectrum. Then, the segments are windowed to reduce spectral leakage. The periodogram of each windowed segment is calculated using the Fourier transform. Finally, the periodograms are averaged to make a single frequency spectrum. In the present study, we have used 50% overlapping and the Hamming window for the spectral density estimation. All data were analyzed using customized software written in Matlab version 9.1 software (Mathworks). The total power of each periodogram was measured as a total index of HRV, which determines the integral of total variability over the entire frequency range. Then, the very low frequency (VLF), the high frequency (HF) and low frequency (LF) components were

extracted. The HF component of HRV (1.5–5 Hz) is predominantly mediated by the phasic activity of the parasympathetic nervous system. The LF oscillations of HR (0.1–1.5 Hz) are regulated by both the sympathetic and parasympathetic nervous systems; however, the tonic sympathetic component is dominant. The VLF component (0-0.1 Hz) is thought to represent reflex changes in HR due to long term blood pressure regulatory mechanisms. Beating interval variability was also assessed using non-linear metrics from Poincaré plot analysis. From these the standard deviations (SD1 and SD2) were calculated using the following equations:

$$SD1^2 = \frac{1}{2}[SD(RR_n - RR_{n+1})]^2$$

$$SD2^2 = 2[SD(RR)]^2 - \frac{1}{2}[SD(RR_n - RR_{n+1})]^2$$